Computers and Concrete, *Vol. 23, No. 3 (2019) 161-170*
DOI: https://doi.org/10.12989/cac.2019.23.3.161

A numerical method for estimating the elastic modulus of recycled concrete

Xinzhu Zhou[a], Jianjun Zheng*, Ting Chen, Jian Zhang, Chuanyang Wang and Jiefeng Wu

School of Civil Engineering and Architecture, Zhejiang University of Technology, Hangzhou 310023, P.R. China

(Received October 14, 2018, Revised March 2, 2019, Accepted March 5, 2019)

Abstract. This paper aims at presenting a numerical method for estimating the elastic modulus of recycled concrete with crushed aggregates. In the method, polygonal aggregates following a given sieve curve are generated, and placed into a square simulation element with the aid of the periodic boundary condition and the overlap criterion of two polygonal aggregates. The mesostructure of recycled concrete is reconstructed by embedding an old interfacial transition zone (ITZ) layer inside each recycled aggregate and by coating all the aggregates with a new ITZ layer. The square simulation element is discretized into a regular grid and a representative point is selected from each sub-element. The iterative method is combined with the fast Fourier transform to evaluate the elastic modulus of recycled concrete. After the validity of the numerical method is verified with experimental results, a sensitivity analysis is conducted to evaluate the effects of key factors on the elastic modulus of recycled concrete. Numerical results show that the elastic modulus of recycled concrete increases with the increase of the total aggregate content and the elastic moduli of old and new ITZ but decreases with increasing the replacement ratio of recycled aggregate and the thicknesses of old and new ITZ. It is also shown that, for a replacement ratio of recycled aggregate smaller than 0.3, the elastic modulus of recycled concrete is reduced by no more than 10%.

Keywords: recycled concrete; elastic modulus; recycled aggregate; fast Fourier transform; crushed aggregate

1. Introduction

Owing to its low cost and high compressive strength, concrete has been widely applied in industrial and civil buildings, hydraulic structures, and roads. With the continuous advancement of China urbanization, the demand for concrete is increasing year by year. The overexploitation of natural sand and stones severely damages mountains and rivers. At the same time, a huge number of concrete structures have been demolished owing to the expiration of their service life, the renewal of old downtown areas, and natural disasters, resulting in a large quantity of waste and serious environmental pollution (Liang *et al.* 2015). In recent years, the development of aggregate recycling techniques and the application of recycled concrete have relieved the increasingly prominent ecological problem to a certain extent. For the application of various recycled concrete structures (Chen *et al.* 2018, Gholamreza *et al.* 2016, Murali *et al.* 2018), it is essential to determine the elastic modulus and to quantify the key influential factors (Duan and Poon 2014).

In the experimental aspect, Ravindrarajah and Tam (1985) investigated the basic properties of recycled aggregate and made clear the difference between recycled and natural aggregate. They concluded that the elastic modulus of recycled aggregate is smaller than that of natural aggregate by up to 30% and suggested an empirical formula of the elastic modulus of recycled concrete. Dhir *et al.* (1999) conducted a comprehensive study on the basic properties of recycled aggregate from different sources and found that, when the contents of recycled coarse and fine aggregate are smaller than 30% and 20%, respectively, they do not exert a significant effect on the elastic modulus. Based on the experimental data, an empirical formula of the elastic modulus of recycled concrete was proposed in terms of the cubic compressive strength. On the basis of previous studies, Xiao *et al.* (2006) analyzed the experimental data on the elastic modulus of recycled concrete and derived a formula of the elastic modulus in the spirit of that of natural aggregate concrete. Kou and Poon (2008) studied the long-term mechanical properties of recycled concrete. They found that, after five years of curing, the elastic modulus decreases with an increase in replacement ratio of recycled aggregate. Compared with recycled aggregates derived from other construction and demolition wastes, concrete made with those derived from pure crushed concrete is of higher elastic modulus. Dapena *et al.* (2011) examined the effect of the recycled sand content on the elastic modulus of recycled concrete and showed that the elastic modulus decreases when concrete is made entirely with recycled aggregate. However, when the replacement ratio of recycled aggregate is smaller than 10%, no appreciable effect on the compressive strength was observed. Dilbas *et al.* (2017) compared the formulae of the elastic modulus of recycled concrete from six standards with experimental results and proposed a new one considering the compressive strength and density. Corinaldesi (2010) designed and tested recycled concrete with a fixed water/cement ratio and 30% replacement ratio of recycled aggregate and related the elastic modulus to the cubic compressive strength. Other

*Corresponding author, Professor
E-mail: jjzheng@zjut.edu.cn
[a]Professor
E-mail: xzzhou66@zjut.edu.cn

http://www.techno-press.org/?journal=cac&subpage=8
ISSN: 1598-8198 (Print), 1598-818X (Online)

similar but slightly different empirical formulae were reported by de Oliveira and Vazquez (1996), Dillmann (1998), Mellmann *et al.* (1999), and Wardeh (2016). To improve the prediction precision and the scope of application, Duan *et al.* (2013) constructed two artificial neural network models using 324 sets of data collected from the literature and 16 more sets of data obtained from their own experiment to predict the elastic modulus of recycled concrete. It was shown that the models could reasonably estimate the elastic modulus of concrete prepared with recycled aggregate derived from different sources. Noguchi *et al.* (2015) analyzed the relationship between the compressive strength and elastic modulus of recycled concrete based on more than 1300 sets of experimental data collected from the literature and proposed a prediction equation of the elastic modulus of recycled concrete considering the replacement ratio and type of recycled aggregate. Based on the quality and replacement ratio of recycled aggregate, Silva *et al.* (2016) conducted a statistical analysis on the experimental data collected from 121 publications and proposed a relationship between the elastic modulus and compressive strength of recycled concrete. Gholampour *et al.* (2017) established a large and reliable test database and derived a new empirical formula for the elastic modulus of recycled concrete, in which the water/cement ratio was taken into account. Golafshni and Behnood (2018) employed four types of soft computing methods to predict the elastic modulus of recycled concrete based on a comprehensive dataset containing 400 sets of experimental data collected from the literature.

In the theoretical aspect, Wang (2013) derived five formulae of the elastic modulus of recycled concrete based on the series model, the parallel model, the Hirsch model, the Counto model, and the Mindess model for two-phase composite materials (Torquato 2002, Hirsh 1962, Du and Jin 2012). It was shown that the later three models have little difference and are of higher prediction precision. Li (2012) modeled recycled concrete as a three-phase material and presented a numerical method for the elastic modulus based on homogenization theory (Torquato 2002). It was demonstrated that the numerical method agrees well with the Mori-Tanaka method (Torquato 2002). Liu (2010) presented a new lattice model to analyze the mechanical properties of recycled concrete. It was shown that the estimated elastic modulus of recycled concrete is in good agreement with experimental results.

From the above literature review, it can be seen that, although great efforts have been made on the elastic modulus of recycled concrete during the past thirty years, these studies have three limitations. First, the empirical formulae are based on limited experimental data and expressed by a simple equation. In fact, recycled concrete is a typical heterogeneous, multi-phase composite material. The content and elastic modulus of each phase and the complex interactions between various phases affect the elastic modulus of recycled concrete, which cannot be reflected through an empirical formula. Second, in existing analytical methods, recycled concrete is usually simplified as a two- or three-phase composite material, consisting of natural aggregate, interfacial transition zone (ITZ), and mortar matrix. This simplification does not distinguish the old mortar and ITZ from the new mortar and ITZ in formulating elastic modulus. Finally, the lattice model can be used to evaluate the elastic modulus of normal and recycled concrete (Liu 2010, Zheng *et al.* 2011). In the model, however, a beam element with three unknown quantities at each edge is adopted. To improve the prediction accuracy, the computer-generated recycled concrete has to be refined, which requires heavy computations. Therefore, it is desirable to develop a numerical method with which the elastic modulus of recycled concrete can be estimated with reasonable accuracy.

The intention of this paper is to develop a numerical algorithm for estimating the elastic modulus of recycled concrete with crushed aggregates. In the algorithm, the mesostructure of recycled concrete is reconstructed and the simulation element is discretized into a regular grid. The iterative method is combined with the fast Fourier transform to evaluate the elastic modulus of recycled concrete. The computational precision of the numerical algorithm is evaluated against experimental results and the key influential factors are quantified through numerical examples.

2. Reconstruction of recycled concrete mesostructure

In practical engineering, recycled aggregates are produced by crushing waste concrete and therefore are generally irregular convex polyhedrons. For the purpose of simulation, it is reasonable to model recycled aggregates as convex polygons in the cross-section of a concrete member. A recycled aggregate is composed of a natural aggregate, old mortar, and an old ITZ layer between them. As such, recycled aggregate has a larger porosity and a lower elastic modulus compared with natural aggregate. To improve its mechanical and transport properties, recycled concrete is usually made with a mixture of recycled and natural aggregate. If the recycled and natural aggregate contents are f_{ra} and f_{na}, respectively, the total aggregate content f_{ta} is equal to $f_{ra}+f_{na}$ and the replacement ratio of recycled aggregate R_{ra} is defined as f_{ra}/f_{ta}. The aggregate size distribution can be obtained from sieve analyses and expressed by a number-based cumulative distribution function $P(d)$. Thus, for a given square simulation element with side a, aggregates can be generated as follows:

1. For polygonal aggregates, the number of sides generally ranges from 3 to 10 (Wang *et al.* 1999). Thus, the number of sides m_i of the i-th aggregate can be determined by

$$m_i = [3 + 8w_{i1}] \tag{1}$$

where w_{i1} is a random number sampled from the uniformly distributed random variable W on [0,1] and $[x]$ is a maximum integer smaller than or equal to x.

2. A polar coordinate system is established at the center o_i. m_i random numbers w_{i2} are sampled from W and arranged from the minimum to the maximum. For the j-th

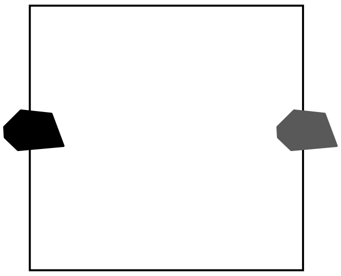

(a)

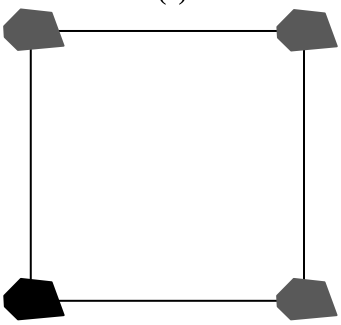

(b)

Fig. 1 When aggregate (black) is located on edge or at vertex, (a) one additional one (grey) and (b) three additional ones (grey) are generated, respectively

vertex of the aggregate, the polar angle θ_i is expressed as

$$\theta_j = 2\pi w_{j2}\ (j = 1, 2, \cdots, m_i) \tag{2}$$

If the polar radius is assumed to vary uniformly from A_1 to A_2, m_i random numbers w_{j3} are sampled from W and the polar radius for the j-th vertex is obtained as

$$r_j = A_1 + (A_2 - A_1) w_{j3}\ (j = 1, 2, \cdots, m_i) \tag{3}$$

3. The aggregate is formed by connecting the neighboring vertexes with a line segment. If the aggregate is concave, it needs to be regenerated by returning to step 2. Otherwise, proceed to the next step.

4. The random number w_{i4} is sampled from W and the size d_i of the aggregate is determined from the following equation

$$P(d_i) = w_{i4} \tag{4}$$

The m_i polar radii of the aggregate are all enlarged or reduced in proportion so that the aggregate size is identical to d_i. The area s_i of the aggregate is computed and the total area S_i of the i aggregates is equal to

$$S_i = S_{(i-1)} + s_i \tag{5}$$

If the condition $S_i \geq f_{ta} a^2$ is satisfied, the generation of aggregates is stopped. Otherwise, return to step 1 to generate the next aggregate.

In order to place these generated aggregates into the square simulation element, they are rearranged from the maximum to the minimum. During the placement, a periodic boundary condition is introduced to avoid any wall effects. If an aggregate (in black) intersects the boundary of the square element, one or three additional aggregates (in grey) are generated by shifting the black aggregate a distance of a along the horizontal and/or vertical directions, as shown in Fig. 1.

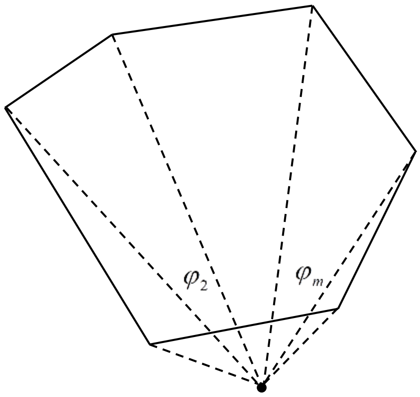

(a)

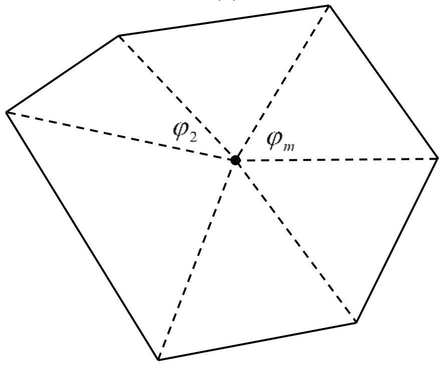

(b)

Fig. 2 Vertex located (a) outside aggregate and (b) inside aggregate

To judge whether two aggregates overlap each other or not, a two-step scheme is adopted. First, each vertex of an aggregate is checked to see whether it falls inside the other aggregates. To this end, the vertex is connected to each one of another aggregate by a line segment and the sum of the included angles between two adjacent line segments is computed. If the sum is smaller than 2π, the vertex is outside the aggregate, as shown in Fig. 2(a). Otherwise, the vertex is inside the aggregate or on an edge of the aggregate, as shown in Fig. 2(b). Second, each edge of an aggregate is checked to see whether it intersects any edge of the other aggregates. This can be achieved by extending the edge and any one of another aggregate to form two straight lines l_1 and l_2 and computing the point of intersection P between them. If the two edges are parallel to each other or the point P falls outside either of the two edges, as shown in Fig. 3(a), they do not intersect. Otherwise, the two aggregates overlap each other, as shown in Fig. 3(b).

With the periodic boundary condition and the overlap criterion of two polygonal aggregates, these generated aggregates can be, one by one, placed into the square element as follows:

1. Two random numbers w_{i5} and w_{i6} are sampled from W and the central coordinates (x_i, y_i) of the i-th aggregate are obtained as

$$x_i = a w_{i5},\quad y_i = a w_{i6} \tag{6}$$

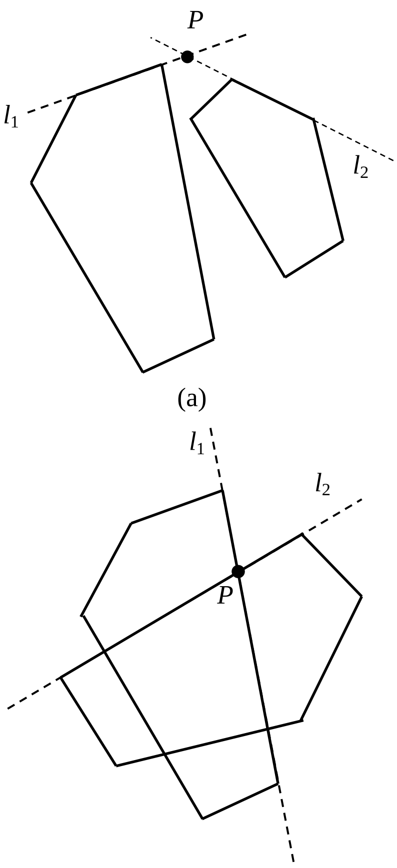

Fig. 3 Point of intersection P between two straight lines l_1 and l_2 falls (a) outside either of two edges and (b) inside at least one of two edges

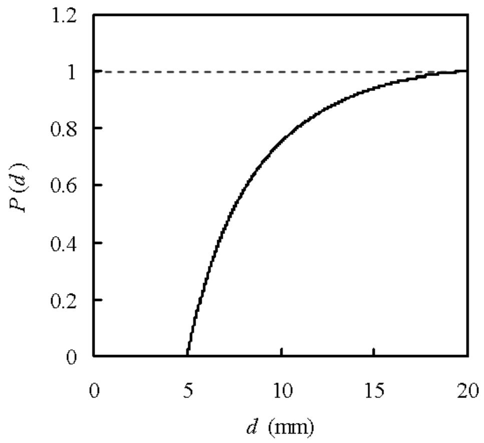

Fig. 4 Fuller aggregate gradation with diameters from 5 to 20 mm

2. If the aggregate intersects the boundary of the square element, the periodic boundary condition is imposed to generate one or three additional aggregates.

3. If there is no overlap between these newly placed aggregates and other ones, steps 1 and 2 are repeated for the next aggregate.

4. Otherwise, discard these newly placed aggregates and return to step 1 to re-locate the aggregate.

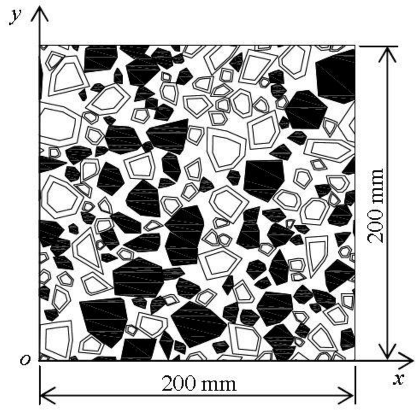

Fig. 5. Simulated distribution of recycled aggregates (white double-polygons) and natural aggregates (black polygons)

As a simulation example, a square element with a side of 200 mm is considered. f_{ta}=0.6, R_{ra}=0.5, and the aggregate size follows the Fuller curve with diameters from 5 to 20 mm. The Fuller aggregate gradation can be expressed as (Zheng *et al*. 2003)

$$P(d) = 1 - \frac{d_{\min}^{1.5} f(\alpha,\beta)}{d^{1.5} f(\alpha_{\min},\beta_{\min})} \tag{7}$$

where $d_{\min}$ and $d_{\max}$ are the minimum and maximum aggregate diameters, respectively; α, $\alpha_{\min}$, β, and $\beta_{\min}$ are given by

$$\alpha = \arccos\left(\frac{d}{d_{\max}}\right), \quad \alpha_{\min} = \arccos\left(\frac{d_{\min}}{d_{\max}}\right) \tag{8}$$

$$\beta = \arcsin\left(\sqrt{2}\sin\frac{\alpha}{2}\right), \quad \beta_{\min} = \arcsin\left(\sqrt{2}\frac{\alpha_{\min}}{2}\right) \tag{9}$$

and $f(\alpha, \beta)$ is defined as

$$\begin{aligned} f(\alpha,\beta) &= -\frac{2}{5}\cos^{1.5}\alpha\sin\alpha \\ &+ \frac{2\sqrt{2}}{5}\left[2E\left(\beta,\frac{1}{\sqrt{2}}\right) - F\left(\beta,\frac{1}{\sqrt{2}}\right)\right] \end{aligned} \tag{10}$$

with $E(\ )$ and $F(\ )$ being the Legendre's standard elliptic integrals (George *et al*. 1999). When $d_{\min}$=5 mm and $d_{\max}$=20 mm, the relationship between $P(d)$ and d is shown in Fig. 4. Thus, the simulated configuration is shown in Fig. 5, where natural and recycled aggregates are represented with black polygons and white double-polygons, respectively. In each recycled aggregate, the inner polygon is the natural aggregate and the zone between the inner and outer polygons is the adhered mortar. It is seen from Fig. 5 that it is quite similar to real concrete.

3. Determination of elastic modulus of recycled concrete

As stated in the previous section, a recycled aggregate consists of a natural aggregate, an old ITZ layer, and old mortar. After recycled concrete is cast, a new ITZ layer is formed between each recycled and natural aggregate and new mortar (Zheng and Zhou 2005). Thus, recycled concrete is, in essence, a five-phase composite material, composed of natural aggregate, old ITZ, old mortar, new ITZ, and new mortar. For such a multi-phase recycled concrete containing polygonal aggregates, it is currently very difficult to derive the elastic modulus in an analytical manner. Therefore, this paper resorts to an effective numerical method as follows.

If the elastic stiffness of reconstructed recycled concrete is expressed in terms of the coordinates (x_1,x_2) as $\boldsymbol{c}_{klmn}(x_1,x_2)$, the stress $\boldsymbol{\sigma}_{kl}(x_1,x_2)$ is related to the strain $\boldsymbol{\varepsilon}_{mn}(x_1,x_2)$ by

$$\boldsymbol{\sigma}_{kl}(x_1,x_2)=\boldsymbol{c}_{klmn}(x_1,x_2)\boldsymbol{\varepsilon}_{mn}(x_1,x_2) \tag{11}$$

When the square simulation element is subjected to no body forces, the governing differential equation is expressed as

$$\boldsymbol{\sigma}_{kl,l}(x_1,x_2)=0 \tag{12}$$

To solve Eqs. (11) and (12), a homogeneous reference material with constant elastic stiffness $\boldsymbol{c}^0_{klmn}$ is introduced. Thus, Eq. (11) can be rewritten as

$$\boldsymbol{\sigma}_{kl}(x_1,x_2)=\boldsymbol{c}^0_{klmn}\boldsymbol{\varepsilon}_{mn}(x_1,x_2)+\boldsymbol{\tau}_{kl}(x_1,x_2) \tag{13}$$

where the polarization tensor $\boldsymbol{\tau}_{kl}(x_1,x_2)$ is defined as

$$\boldsymbol{\tau}_{kl}(x_1,x_2)=(\boldsymbol{c}_{klmn}(x_1,x_2)-\boldsymbol{c}^0_{klmn})\boldsymbol{\varepsilon}_{mn}(x_1,x_2) \tag{14}$$

With the periodic Green operator $\boldsymbol{\Gamma}^0_{klmn}(x_1,x_2)$, the solution to Eqs. (12) and (13) is given by (Moulinec and Suquet 1998)

$$\boldsymbol{\varepsilon}_{kl}(x_1,x_2)=-\boldsymbol{\Gamma}^0_{klmn}(x_1,x_2)*\boldsymbol{\tau}_{mn}(x_1,x_2) \tag{15}$$

where "*" denotes the convolution operator. The Fourier transform of Eq. (15) is

$$\bar{\boldsymbol{\varepsilon}}_{kl}(\xi_1,\xi_2)=-\bar{\boldsymbol{\Gamma}}^0_{klmn}(\xi_1,\xi_2)\bar{\boldsymbol{\tau}}_{mn}(\xi_1,\xi_2) \tag{16}$$

where $\bar{\boldsymbol{\Gamma}}^0_{klmn}(\xi_1,\xi_2)$ is expressed in terms of the Lamé coefficients λ^0 and μ^0 of the reference material as (Moulinec and Suquet 1998)

$$\boldsymbol{\Gamma}^0_{klmn}(\xi_1,\xi_2)=\frac{(\boldsymbol{\delta}_{mk}\xi_n\xi_l+\boldsymbol{\delta}_{nk}\xi_m\xi_l+\boldsymbol{\delta}_{ml}\xi_n\xi_k+\boldsymbol{\delta}_{nl}\xi_m\xi_k)}{4\mu^0(\xi_1^2+\xi_2^2)} \\ -\frac{(\lambda^0+\mu^0)\xi_k\xi_l\xi_m\xi_n}{\mu^0(\lambda^0+2\mu^0)(\xi_1^2+\xi_2^2)^2} \tag{17}$$

with $\boldsymbol{\delta}_{kl}$ being the Kronecker delta.

It was shown that the ITZ thickness is seldom influenced by the aggregate size (Scrivener and Nemati 1996). Thus, the mesostructure of recycled concrete can be reconstructed as follows. In the simulated distribution of aggregates, each recycled and natural aggregate is coated with a new ITZ layer of thickness h_{ni}, as shown in Fig. 6. For each recycled aggregate, adhered mortar is composed of an old ITZ layer and old mortar. The content of adhered mortar m_{am} can be measured by experiment (Liu 2010). Since there is at present a lack of further information on recycled aggregate, it is assumed in this paper that the

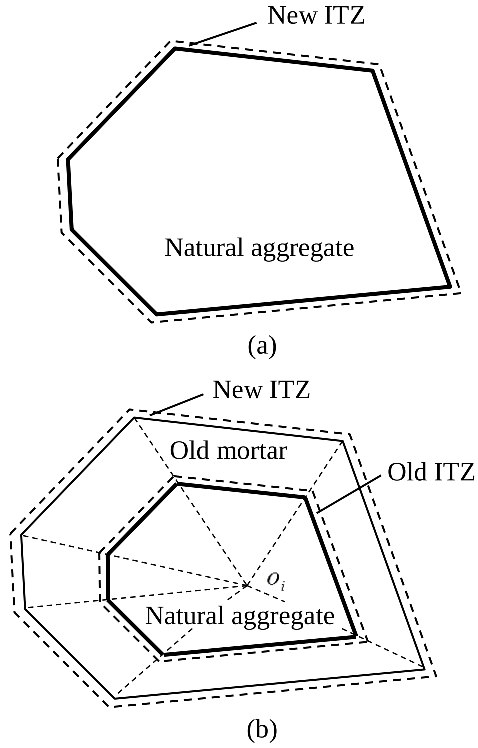

Fig. 6 Geometrical relationships among various phases for (a) natural aggregate and (b) recycled aggregate

content of adhered mortar is the same for each recycled aggregate and the natural aggregate in the recycled aggregate is homothetic to the recycled aggregate with respect to the center o_i as a preliminary study. Thus, a point is found on each polar radius so that the distance from the point to the center o_i is equal to $\sqrt{1-m_{am}^2}r_j$. Each two points on the neighboring polar radii are then connected with a segment line to form a natural aggregate. Finally, the natural aggregate in the recycled aggregate is coated with an old ITZ layer with thickness h_{oi}, as shown in Fig. 6(b).

To increase the computational efficiency, a radix-2 fast Fourier transform is adopted in this paper. For this reason, the square simulation element is discretized into a regular grid composed of $2^M\times2^M$ sub-elements, as shown in Fig. 7. For each sub-element, the center is selected as the representative point. Each representative point is endowed with the elastic stiffness of the phase inside which it falls. For example, if the representative point is located within a certain natural aggregate, its elastic stiffness is equal to that of natural aggregate. As expected, a larger value of M represents a more detailed mesostructure of recycled concrete and therefore results in a more accurate elastic modulus, but more data need to be stored and a longer computational time is required. For the simulated mesostructure shown in Fig. 7, the aggregate size follows the Fuller curve, the smallest and largest aggregate diameters are 5 and 20 mm, respectively, f_{ta}=0.6, R_{ra}=0.5, m_{am}=0.5, h_{oi}=0.045 mm, and h_{ni}=0.060 mm. When M=8, the square simulation element is discretized into $2^8\times2^8$=256×256 sub-elements. Thus, there are 65536 representative points in total. The number of representative

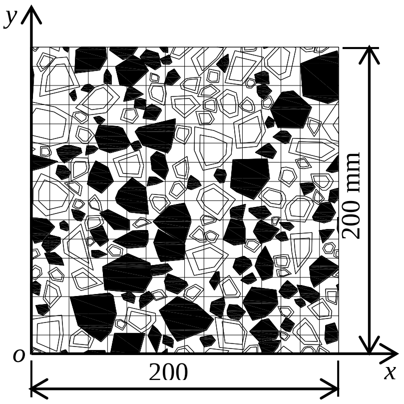

Fig. 7 Discretization of square simulation element

Table 1 Number of representative points in and content of each phase in mesostructure of recycled concrete shown in Fig. 7

Phase	Number of representative points	Content
Natural aggregate	29278	0.447
Old mortar	9505	0.145
Old ITZ	173	0.003
New mortar	25910	0.395
New ITZ	670	0.010

points that fall within each phase is computed as shown in Table 1. Since part of natural aggregates are included in recycled aggregates, the natural aggregate content is 0.45. The adhered mortar consists of the old mortar and the old ITZ and the content is 0.15. The content of the new mortar and the new ITZ is 1−0.45−0.15=0.4. As can be seen from Table 1, the three contents are very close to 0.447, 0.148, and 0.405, respectively. Therefore, when M=8, the representative points are accurate enough to describe the simulated mesostructure of recycled concrete. Furthermore, it will be seen in the next section that the estimated elastic modulus of recycled concrete is also of high enough precision. When M =8, the coordinates of the i-th vertical line segment and the j-th horizontal line segment are 25(i−1)/32 (i=1,2,…,257) and 25(j−1)/32 (j=1,2,…,257), respectively. Thus, the coordinates of the corner points and representative point in each sub-element can be easily determined.

The elastic modulus of recycled concrete is estimated with the iterative method as follows (Moulinec and Suquet 1998):

1. An initial uniform strain $\boldsymbol{\varepsilon}_{kl}^{(0)}$ in the x_1 direction is assigned to each representative point. From Eq. (11), the initial stresses $\boldsymbol{\sigma}_{kl}^{(0)}(x_1, x_2)$ at these representative points are calculated.

2. At step $i+1$, $\bar{\boldsymbol{\varepsilon}}_{kl}^{(i)}(\xi_1, \xi_2)$ and $\bar{\boldsymbol{\sigma}}_{kl}^{(i)}(\xi_1, \xi_2)$ are calculated from $\boldsymbol{\varepsilon}_{kl}^{(i)}(x_1, x_2)$ and $\boldsymbol{\sigma}_{kl}^{(i)}(x_1, x_2)$ through the fast Fourier transform, respectively (Rao *et al*. 2010). If the relative error at each representative point $\left|\bar{\boldsymbol{\sigma}}_{kl}^{(i)}(\xi_1, \xi_2) - \bar{\boldsymbol{\sigma}}_{kl}^{(i-1)}(\xi_1, \xi_2)\right| / \left|\bar{\boldsymbol{\sigma}}_{kl}^{(i)}(\xi_1, \xi_2)\right|$ is all smaller than a prescribed value (0.001 in this paper), stop the iterative procedure and jump to step 4. Otherwise, proceed to the next step.

3. From Eq. (14), $\boldsymbol{\tau}_{kl}^{(i)}(x_1, x_2)$ is calculated and $\bar{\boldsymbol{\tau}}_{kl}^{(i)}(\xi_1, \xi_2)$ is then obtained from the fast Fourier transform. Substitution of $\bar{\boldsymbol{\tau}}_{kl}^{(i)}(\xi_1, \xi_2)$ into the right-hand side of Eq. (16) yields $\bar{\boldsymbol{\varepsilon}}_{kl}^{(i+1)}(\xi_1, \xi_2)$. $\boldsymbol{\varepsilon}_{kl}^{(i+1)}(x_1, x_2)$ is then obtained from the inverse fast Fourier transform. Go back to step 2.

4. The area-weighted average strain and stress in the x_1 direction are calculated and the elastic modulus of recycled concrete is equal to the ratio between the average stress and the average strain.

4. Experimental verification and discussions

To assess the prediction precision of the numerical algorithm, two sets of test data are obtained from the literature: one is for normal concrete and the other is for recycled concrete.

First, we choose the experimental results of normal concrete conducted by Stock *et al*. (1979). In the test, four types of concrete specimens with a water/cement ratio of 0.5 and aggregate contents of 0.2, 0.4, 0.6, and 0.8 were cast. The largest size and elastic modulus of natural aggregate were 19 mm and 75.5 GPa, respectively. The elastic modulus of cement paste matrix was measured as 11.6 GPa. Since no recycled aggregates are added to the normal concrete, it only includes three phases: natural aggregate, ITZ, and cement paste matrix. To evaluate the elastic modulus, Poisson’s ratios of the three components, and the thickness and elastic modulus of ITZ need to be estimated. According to the quantitative analysis of Zheng *et al*. (2006), the ITZ thickness may be taken as 0.03 mm, the elastic modulus of ITZ is around 60% of that of cement paste matrix, and Poisson’s ratios of natural aggregate, cement paste matrix, and ITZ are approximately set to be 0.15, 0.25, and 0.35, respectively. With these parameters known, the elastic modulus of concrete is calculated using

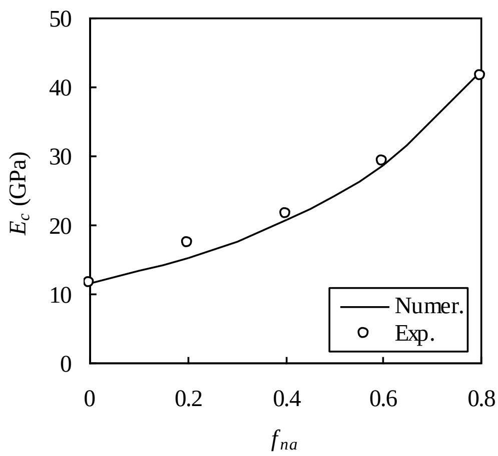

Fig. 8 Comparison between numerical method and experimental results of Stock *et al*. (1979)

Table 2 Aggregate size distributions for RA1 and RA2

Sieve size (mm)	Cumulative percentage passing (%)	
	RA1	RA1
25.0	100	100
20.0	82.9	83.5
16.5	64.2	65.3
10.0	30.9	33.1
5.0	0	0

Table 3 Elastic modulus of each phase constituent

Phase constituent	Elastic modulus (GPa)
Natural aggregate	80
Old mortar in RA1	19.27
Old mortar in RA2	23.17
New mortar in M1	23.68
New mortar in M2	26.52

Table 4 Comparison with experimental results of Liu (2010)

Type	RC1	RC2	RC3	RC4
Exp. (GPa)	29.49	32.79	29.52	32.38
Numer. (GPa)	29.39	31.13	30.85	32.20
Relative error (%)	0.34	5.1	4.5	0.56

the proposed numerical method as shown in Fig. 8, together with the experimental results. It is calculated that, when f_{na} is 0.2, 0.4, 0.6, and 0.8, the relative error between them is 12%, 3.4%, 1.5%, and 1.9%, respectively.

Second, we consider the experimental results of recycled concrete obtained by Liu (2010). In his experiment, two mixes, denoted by M1 and M2, were designed. The proportions of cement, river sand, recycled coarse aggregate, and water were 1.000: 1.989: 3.693: 0.574 for M1 and 1.000: 1.395: 2.592: 0.429 for M2. Two types of recycled aggregate, denoted by RA1 and RA2, were adopted. Their size distributions are shown in Table 2. The content of adhered mortar and apparent density were 42.2% and 2415 kg/m^3 for RA1 and 46.5% and 2429 kg/m^3 for RA2, respectively. Four types of recycled concrete, denoted by RC1, RC2, RC3, and RC4, were made and tested by combining different mixes and types of recycled aggregate, i.e., M1+RA1, M2+RA1, M1+RA2, and M2+RA2. The elastic modulus of each phase constituent is shown in Table 3. The thicknesses of old and new ITZ were 0.045 and 0.060 mm, respectively (Xiao *et al*. 2013). In the numerical analysis, the elastic modulus of ITZ is assumed to be 60% of that of the corresponding mortar. Since Poisson's ratios of various phases vary slightly and have a marginal effect on the elastic modulus of recycled concrete, they are all taken as 0.2. Thus, a comparison between the experimental results and numerical predictions is made in Table 4. The relative error between them is 0.34%, 5.1%, 4.5%, and 0.56% for RC1, RC2, RC3, and RC4, respectively. Therefore, the numerical method can estimate the elastic modulus of recycled concrete with reasonable accuracy.

It is seen from the above numerical method that the elastic modulus of recycled concrete is affected by various factors. Therefore, it is of interest to quantify them based on

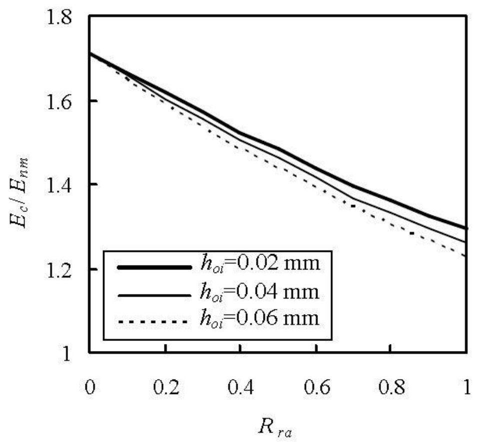

Fig. 9 Effects of old ITZ thickness and replacement ratio of recycled aggregate on elastic modulus of recycled concrete

numerical analyses. In the following computations, the coarse aggregate size follows the Fuller curve with sizes from 5 to 16 mm. Poisson's ratios of various phases are equal to 0.2. In the recycled aggregate, the content of adhered mortar is 0.5. For convenience, the elastic modulus of each phase is given relative to that of new mortar E_{nm}. The relative elastic moduli of natural aggregate and old mortar are fixed as 3.0 and 0.9, respectively.

4.1 Effects of old ITZ thickness and replacement ratio of recycled aggregate

For this purpose, the total aggregate content is 0.5, the new ITZ thickness is 0.06 mm, and the relative elastic moduli of old and new ITZ are 0.5 and 0.6, respectively. With these parameters, the relative elastic modulus of recycled concrete E_c/E_{nm} is plotted against R_{ra} as shown in Fig. 9 for different h_{oi}. It is shown from Fig. 9 that, for a given h_{oi}, E_c/E_{nm} decreases with the increase of R_{ra}. Since the old mortar is less stiff than the new one, a larger R_{ra} results in a larger content of adhered mortar and a lower elastic modulus. When R_{ra} increases from 0 to 0.3, E_c/E_{nm} decreases by 8.0%, 9.0%, and 10% for h_{oi}=0.02, 0.04, and 0.06 mm, respectively. This indicates that, when the replacement ratio of recycled aggregate is not beyond 0.3, the decrease ratio of the elastic modulus is smaller than 10%. However, when R_{ra} varies from 0 to 1, E_c/E_{nm} reduces by 24%, 26%, and 28% for h_{oi}= 0.02, 0.04, and 0.06 mm, respectively. As expected, E_c/E_{nm} decreases with increasing h_{oi} for a given R_{ra}. When R_{ra}=0.2, 0.4, 0.6, 0.8, and 1.0, E_c/E_{nm} at h_{oi} =0.06 mm is smaller than that at h_{oi}=0.02 mm by 2.1%, 2.4%, 3.2%, 4.4%, and 5.3%, respectively.

4.2 Effect of elastic modulus of old ITZ

The effect of the elastic modulus of old ITZ E_{oi} on that of recycled concrete is shown in Fig. 10, where the total aggregate content is 0.5, the relative elastic modulus of new ITZ is 0.6, and the thickness is 0.045 and 0.060 mm for old and new ITZ, respectively. Fig. 10 demonstrates that, for a given R_{ra}, E_c/E_{nm} decreases as E_{oi}/E_{nm} decreases.

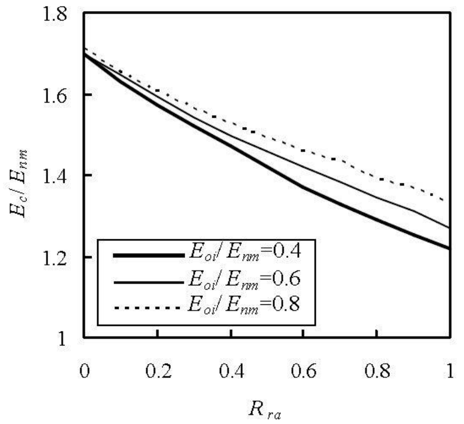

Fig. 10 Effect of elastic modulus of old ITZ on elastic modulus of recycled concrete

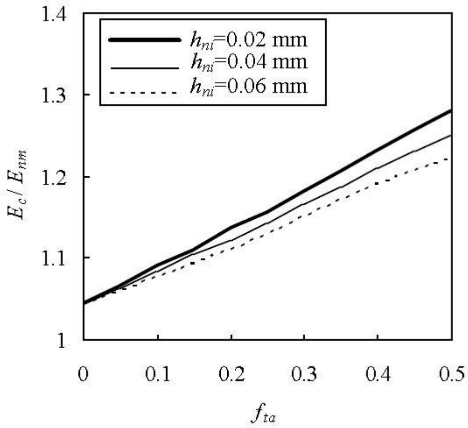

Fig. 11 Effects of new ITZ thickness and total aggregate content on elastic modulus of recycled concrete

Specifically, when R_{ra} =0.2, 0.4, 0.6, 0.8, and 1.0, E_c/E_{nm} at E_{oi}/E_{nm}=0.4 is smaller than that at E_{oi}/E_{nm}=0.8 by 2.1%, 3.6%, 6.0%, 7.3%, and 8.7%, respectively.

4.3 Effects of new ITZ thickness and total aggregate content

It should be noted that only the coarse aggregate is considered as an independent phase in this paper, while the fine aggregate is included in the mortar. Generally, the division between coarse and fine aggregate is 5 mm. If the Fuller gradation is considered, the largest aggregate diameter is set to be 20 mm, and the content of coarse and fine aggregate is 0.8, the content of coarse aggregate is equal to 0.44, 0.46, and 0.48 for a given smallest aggregate diameter at 0.15, 0.30, and 0.60 mm, respectively. Therefore, the maximum value of f_{ta} is taken as 0.5 in the following computations. The replacement ratio of recycled aggregate is 1.0, the thickness of old ITZ is 0.045 mm, and the relative elastic modulus is 0.5 and 0.6 for old and new ITZ, respectively, to analyze the effects of the new ITZ thickness h_{ni} and the total aggregate content f_{ta} on the elastic modulus of recycled concrete. The results are shown in Fig. 11, which shows that, for a given h_{ni}, E_c/E_{nm} is an increasing function of f_{ta}. Since the natural aggregate is of the highest

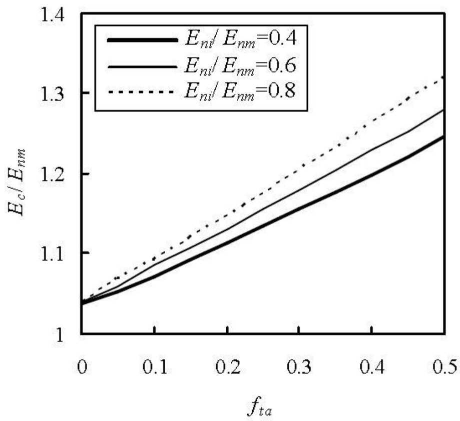

Fig. 12 Effect of elastic modulus of new ITZ on elastic modulus of recycled concrete

elastic modulus among these phases. A larger aggregate content results in a larger natural aggregate content and therefore a higher elastic modulus of recycled concrete. Specifically, When f_{ta} increases from 0 to 0.5, E_c/E_{nm} increases by 17%, 20%, and 23% for h_{ni}=0.02, 0.04, and 0.06 mm, respectively. Fig. 11 also shows that, for a given f_{ta}, E_c/E_{nm} decreases with the increase of h_{ni}. When f_{ta} is 0.1, 0.2, 0.3, 0.4, and 0.5, E_c/E_{nm} at h_{ni}=0.06 mm is smaller than that at h_{ni}=0.02 mm by 1.4%, 2.3%, 2.7%, 3.4%, and 4.7%, respectively.

4.4 Effect of elastic modulus of new ITZ

The effect of the elastic modulus of new ITZ E_{ni} on that of recycled concrete is shown in Fig. 12, where the replacement ratio of recycled aggregate is 1.0, the relative elastic modulus of old ITZ is 0.5, and the thickness is 0.045 and 0.060 mm for old and new ITZ, respectively. Fig. 12 demonstrates that E_c/E_{nm} decreases with decreasing E_{ni}/E_{nm} for a given f_{ta}. When f_{ta}=0.1, 0.2, 0.3, 0.4, and 0.5, E_c/E_{nm} at E_{ni}/E_{nm}=0.4 is smaller than that at E_{ni}/E_{nm}=0.8 by 1.9%, 2.9%, 4.1%, 5.1%, and 5.7%, respectively.

From the above sensitivity analysis, it is seen that the most important factor is the replacement ratio of recycled aggregate. When R_{ra} increases from 0 to 1, E_c/E_{nm} decreases by 24% to 28%. The second most important factor is the total aggregate content. When f_{ta} increases from 0 to 0.5, E_c/E_{nm} increases by 17% to 23%. The least important factors are the thicknesses and elastic moduli of old and new ITZ. The extent to which they influence the elastic modulus of recycled concrete is in the range of 1.4% to 8.7%.

5. Conclusions

A numerical algorithm has been presented for estimating the elastic modulus of recycled concrete with crushed aggregates. With the aid of computer simulation, the five-phase mesostructure of recycled concrete has been reconstructed. The simulated mesostructure has been discretized into a series of sub-elements. For each sub-element, a representative point has been selected and endowed with the elastic stiffness of the phase inside which the point falls. A fast Fourier transform based iterative method has been adopted to estimate the elastic modulus of recycled concrete. A comparison with the experimental results of normal and recycled concrete has validated the numerical method. Several examples have been implemented to quantify the key influential factors. It has been shown that the replacement ratio of recycled aggregate is the most important factor. When it varies from 0 to 1, the elastic modulus decreases by 24% to 28%. The total aggregate content is the second most important factor. When it varies from 0 to 0.5, the elastic modulus increases by 17% to 23%. The thicknesses and elastic moduli of old and new ITZ are the least important factors. The extent to which they influence the elastic modulus is between 1.4% and 8.7%.

Acknowledgments

The financial support from the National Natural Science Foundation (Grant Nos. 51878615 and 51779227) and the Open Research Fund Program of State key Laboratory of Hydroscience and Engineering (Grant No. sklhse-2019-C-01), of the People's Republic of China, is gratefully acknowledged.

References

Chen, X.D., Shen, N., Tian, H.X., Fan, X.Q. and Lu, J. (2018), “Mechanical properties of pervious concrete with recycled aggregate”, *Comput. Concrete*, **21**(6), 621-635.

Corinaldesi, V. (2010), “Mechanical and elastic behavior of concretes made of recycled-concrete coarse aggregates”, *Constr. Build. Mater.*, **24**(9), 1616-1620.

Dapena, E., Alaejos, P., Lobet, A. and Pérez, D. (2011), “Effect of recycled sand content on characteristics of mortars and concretes”, *J. Mater. Civil Eng.*, **23**(4), 414-422.

de Oliveira, M.B. and Vazquez, E. (1996), “The influence of retained moisture in aggregates from recycling on the properties of new hardened concrete”, *Waste Manage.*, **16**(1-3), 113-117.

Dhir, R.K., Limbachiya, M.C. and Leelawat, T. (1999), “Suitability of recycled aggregate for use in BS 5328 designated mixes”, *Proc. Inst. Civ. Eng. Struct. Build.*, **134**(3), 257-274.

Dilbas, H., Cakir, Ö. and Simsek, M. (2017), “Recycled aggregate concretes (RACs) for structural use: an evaluation on elasticity modulus and energy capacities”, *Int. J. Civil Eng.*, **15**(2), 1-15.

Dillmann, R. (1998), “Concrete with recycled concrete aggregate”, *Proceedings of the International Symposium on Sustainable Construction: Use of Recycled Concrete Aggregate*, London, UK, January.

Du, X.L. and Jin, L. (2012), “Research on effective mechanical properties of concrete composite material with pores”, *Eng. Mech.*, **29**(8), 70-77. (in Chinese)

Duan, Z.H. and Poon, C.S. (2014), “Factors affecting the properties of recycled concrete by using neural networks**”,** *Comput. Concrete*, **14**(5), 547-561.

Duan, Z.H., Kou, S.C. and Poon, C.S. (2013), “Using artificial neural networks for predicting the elastic modulus of recycled aggregate concrete”, *Constr. Build. Mater.*, **44**(7), 524-532.

George, E.A., Richard, A. and Ranjan, R. (1999), *Special Function*, Cambridge University Press, Cambridge, UK.

Gholampour, A., Gandomi, A.H. and Ozbakkaloglu, T. (2017), “New formulations for mechanical properties of recycled aggregate concrete using gene expression programming”, *Constr. Build. Mater.*, **130**, 122-145.

Gholamreza, A., Ehsan, J. and Zahra, K. (2016), “Predicting of compressive strength of recycled aggregate concrete by genetic programming”, *Comput. Concrete*, **18**(2), 155-164.

Golafshni, E.M. and Behnood, A. (2018), “Application of soft computing methods for predicting the elastic modulus of recycled aggregate concrete”, *J. Clean. Prod.*, **176**, 1163-1176.

Hirsh, T.J. (1962), “Modulus of elasticity of concrete affected by elastic moduli of cement paste matrix and aggregate”, *J. Am. Concr. Inst.*, **59**(3), 427-452.

Kou, S.C. and Poon, C.S. (2008), “Mechanical properties of 5-year-old concrete prepared with recycled aggregates obtained from three different sources”, *Mag. Concr. Res.*, **60**(1), 57-64.

Li, B.D. (2012), “Mesoscopic analysis and numerical simulation of mechanical properties for recycled concrete composite materials with interface”, Master Dissertation, South China University of Technology, Guangzhou, China. (in Chinese)

Liang, J.F., Yang, Z.P., Yi, P.H. and Wang, J.B. (2015) “Mechanical properties of recycled fine glass aggregate concrete under uniaxial loading”, *Comput. Concrete*, **16**(2), 275-285.

Liu, Q. (2010), “The experimental study and lattice model simulation on the failure mechanism of recycled concrete”, Ph.D. Dissertation, Tongji University, Shanghai, China. (in Chinese)

Mellmann, G., Meinhold, U. and Maultzsch, M. (1999), “Processed concrete rubble for the reuse as aggregate”, *Proceedings of the International Seminar on Exploiting Wastes in Concrete*, Dundee, UK, September.

Moulinec, H. and Suquet, P. (1998), “A numerical method for computing the overall response of nonlinear composites with complex microstructure”, *Comput. Meth. Appl. Mech. Eng.*, **157**(1-2), 69-94.

Murali, G., Indhumathi, T., Karthikeyan, K. and Ramkumar, V.R. (2018), “Analysis of flexural fatigue failure of concrete made with 100% coarse recycled and natural aggregates”, *Comput. Concrete*, **21**(3), 291-298.

Noguchi, T., Park, W.J., Oh, D.Y. and Shin, S.H. (2015), “Modulus of elasticity of recycled aggregate concrete”, *Mag. Concrete Res.*, **67**(11), 585-591.

Rao, K.R., Kim, D.N. and Hwang, J.J. (2010), *Fast Fourier Transforms: Algorithms and Applications*, Springer, Dordrecht, the Netherlands.

Ravindrarajah, R.S. and Tam, C.T. (1985), “Properties of concrete made with crushed concrete as coarse aggregate”, *Mag. Concrete Res.*, **37**(130), 29-38.

Scrivener, K.L. and Nemati, K.M. (1996), “The percolation of pore space in the cement paste/aggregate interfacial zone of concrete”, *Cement Concrete Res.*, **26**(1), 35-40.

Silva, R.V., de Brito, J. and Dhir, R.K. (2016), “Establishing a relationship between modulus of elasticity and compressive strength of recycled aggregate concrete”, *J. Clean. Prod.*, **112**, 2171-2186.

Stock, A.F., Hannant, D.J. and Williams, R.I.T. (1979), “The effect of aggregate concentration upon the strength and modulus of elasticity of concrete”, *Mag. Concrete Res.*, **31**(113), 225-234.

Torquato, S. (2002), *Random Heterogenerous Materials: Microstructure and Macroscopic Properties*, Springer, New York, USA.

Wang, H.L. (2013), “Study on elastic modulus of recycled aggregate concrete”, *J. Dalian Univ.*, **34**(3), 45-49. (in Chinese)

Wang, Z.W., Kwan, A.K.W. and Chan, H.C. (1999), “Mesoscopic study of concrete I: generation of random aggregate structure and finite element mesh”, *Comput. Struct.*, **70**(5), 533-544.

Wardeh, G., Ghorbel, E. and Gomart, H. (2015), "Mix design and properties of recycled aggregate concretes: applicability of eurocode 2", *Int. J. Concrete Struct. Mater.*, **9**(1), 1-20.

Xiao, J.Z., Li, J.B. and Zhang, C. (2006),"On relationships between the mechanical properties of recycled aggregate concrete: an overview", *Mater. Struct.*, **39**(6), 655-664.

Xiao, J.Z., Li, W.G., Sun, Z.H., Lange, D.A. and Shah, S.P. (2013), "Properties of interfacial transition zones in recycled aggregate concrete tested by nanoindentation", *Cement Concrete Compos.*, **37**(3), 276-292.

Zheng, J.J., Li, C.Q. and Zhao, L.Y. (2003), "Simulation of two-dimensional aggregate distribution with wall effect", *J. Mater. Civil Eng.*, **15**(5), 506-510.

Zheng, J.J., Li, C.Q. and Zhou, X.Z. (2005), "Thickness of interfacial transition zone and cement content profiles around aggregates", *Mag. Concrete Res.*, **57**(7), 397-406.

Zheng, J.J., Li, C.Q. and Zhou, X.Z. (2006), "An analytical method for prediction of the elastic modulus of concrete", *Mag. Concrete Res.*, **58**(10), 665-673.

Zheng, J.J., Zhou, X.Z., Wu, Z.M. and Jin, X.Y. (2011), "Numerical method for predicting Young's modulus of concrete with aggregate shape effect", *J. Mater. Civil Eng.*, **23**(10), 1609-1615.

CC